GEORGIAN MEDICAL NEWS

ISSN 1512-0112

NO 3 (372) Март 2026

ТБИЛИСИ - NEW YORK

ЕЖЕМЕСЯЧНЫЙ НАУЧНЫЙ ЖУРНАЛ

Медицинские новости Грузии

საქართველოს სამედიცინო სიახლენი

GEORGIAN MEDICAL NEWS

Monthly Georgia-US joint scientific journal published both in electronic and paper formats of the Agency of Medical Information of the Georgian Association of Business Press. Published since 1994. Distributed in NIS, EU and USA.

GMN: Georgian Medical News is peer-reviewed, published monthly journal committed to promoting the science and art of medicine and the betterment of public health, published by the GMN Editorial Board since 1994. GMN carries original scientific articles on medicine, biology and pharmacy, which are of experimental, theoretical and practical character; publishes original research, reviews, commentaries, editorials, essays, medical news, and correspondence in English and Russian.

GMN is indexed in MEDLINE, SCOPUS, PubMed and VINITI Russian Academy of Sciences. The full text content is available through EBSCO databases.

GMN: Медицинские новости Грузии - ежемесячный рецензируемый научный журнал, издаётся Редакционной коллегией с 1994 года на русском и английском языках в целях поддержки медицинской науки и улучшения здравоохранения. В журнале публикуются оригинальные научные статьи в области медицины, биологии и фармации, статьи обзорного характера, научные сообщения, новости медицины и здравоохранения. Журнал индексируется в MEDLINE, отражён в базе данных SCOPUS, PubMed и ВИНИТИ РАН. Полнотекстовые статьи журнала доступны через БД EBSCO.

GMN: Georgian Medical News – საქართველოს სამედიცინო სიახლენი – არის ყოველთვიური სამეცნიერო სამედიცინო რეცენზირებადი ჟურნალი, გამოიცემა 1994 წლიდან, წარმოადგენს სარედაქციო კოლეგიისა და აშშ-ის მეცნიერების, განათლების, ინდუსტრიის, ხელოვნებისა და ბუნებისმეტყველების საერთაშორისო აკადემიის ერთობლივ გამოცემას. GMN-ში რუსულ და ინგლისურ ენებზე ქვეყნდება ექსპერიმენტული, თეორიული და პრაქტიკული ხასიათის ორიგინალური სამეცნიერო სტატიები მედიცინის, ბიოლოგიისა და ფარმაციის სფეროში, მიმოხილვითი ხასიათის სტატიები.

ჟურნალი ინდექსირებულია MEDLINE-ის საერთაშორისო სისტემაში, ასახულია SCOPUS-ის, PubMed-ის და ВИНИТИ РАН-ის მონაცემთა ბაზებში. სტატიების სრული ტექსტი ხელმისაწვდომია EBSCO-ს მონაცემთა ბაზებიდან.

WEBSITE

www.geomednews.com

К СВЕДЕНИЮ АВТОРОВ!

При направлении статьи в редакцию необходимо соблюдать следующие правила:

1. Статья должна быть представлена в двух экземплярах, на русском или английском языках, напечатанная через **полтора интервала на одной стороне стандартного листа с шириной левого поля в три сантиметра**. Используемый компьютерный шрифт для текста на русском и английском языках - **Times New Roman** (**Кириллица**), для текста на грузинском языке следует использовать **AcadNusx.** Размер шрифта - **12**. К рукописи, напечатанной на компьютере, должен быть приложен CD со статьей.

2. Размер статьи должен быть не менее десяти и не более двадцати страниц машинописи, включая указатель литературы и резюме на английском, русском и грузинском языках.

3. В статье должны быть освещены актуальность данного материала, методы и результаты исследования и их обсуждение.

При представлении в печать научных экспериментальных работ авторы должны указывать вид и количество экспериментальных животных, применявшиеся методы обезболивания и усыпления (в ходе острых опытов).

4. К статье должны быть приложены краткое (на полстраницы) резюме на английском, русском и грузинском языках (включающее следующие разделы: цель исследования, материал и методы, результаты и заключение) и список ключевых слов (key words).

5. Таблицы необходимо представлять в печатной форме. Фотокопии не принимаются. **Все цифровые, итоговые и процентные данные в таблицах должны соответствовать таковым в тексте статьи**. Таблицы и графики должны быть озаглавлены.

6. Фотографии должны быть контрастными, фотокопии с рентгенограмм - в позитивном изображении. Рисунки, чертежи и диаграммы следует озаглавить, пронумеровать и вставить в соответствующее место текста **в tiff формате**.

В подписях к микрофотографиям следует указывать степень увеличения через окуляр или объектив и метод окраски или импрегнации срезов.

7. Фамилии отечественных авторов приводятся в оригинальной транскрипции.

8. При оформлении и направлении статей в журнал МНГ просим авторов соблюдать правила, изложенные в «Единых требованиях к рукописям, представляемым в биомедицинские журналы», принятых Международным комитетом редакторов медицинских журналов - http://www.spinesurgery.ru/files/publish.pdf и http://www.nlm.nih.gov/bsd/uniform_requirements.html
В конце каждой оригинальной статьи приводится библиографический список. В список литературы включаются все материалы, на которые имеются ссылки в тексте. Список составляется в алфавитном порядке и нумеруется. Литературный источник приводится на языке оригинала. В списке литературы сначала приводятся работы, написанные знаками грузинского алфавита, затем кириллицей и латиницей. Ссылки на цитируемые работы в тексте статьи даются в квадратных скобках в виде номера, соответствующего номеру данной работы в списке литературы. Большинство цитированных источников должны быть за последние 5-7 лет.

9. Для получения права на публикацию статья должна иметь от руководителя работы или учреждения визу и сопроводительное отношение, написанные или напечатанные на бланке и заверенные подписью и печатью.

10. В конце статьи должны быть подписи всех авторов, полностью приведены их фамилии, имена и отчества, указаны служебный и домашний номера телефонов и адреса или иные координаты. Количество авторов (соавторов) не должно превышать пяти человек.

11. Редакция оставляет за собой право сокращать и исправлять статьи. Корректура авторам не высылается, вся работа и сверка проводится по авторскому оригиналу.

12. Недопустимо направление в редакцию работ, представленных к печати в иных издательствах или опубликованных в других изданиях.

При нарушении указанных правил статьи не рассматриваются.

REQUIREMENTS

Please note, materials submitted to the Editorial Office Staff are supposed to meet the following requirements:

1. Articles must be provided with a double copy, in English or Russian languages and typed or compu-ter-printed on a single side of standard typing paper, with the left margin of **3** centimeters width, and **1.5** spacing between the lines, typeface - **Times New Roman** (**Cyrillic**), print size - **12** (referring to Georgian and Russian materials). With computer-printed texts please enclose a CD carrying the same file titled with Latin symbols.

2. Size of the article, including index and resume in English, Russian and Georgian languages must be at least 10 pages and not exceed the limit of 20 pages of typed or computer-printed text.

3. Submitted material must include a coverage of a topical subject, research methods, results, and review.

Authors of the scientific-research works must indicate the number of experimental biological species drawn in, list the employed methods of anesthetization and soporific means used during acute tests.

4. Articles must have a short (half page) abstract in English, Russian and Georgian (including the following sections: aim of study, material and methods, results and conclusions) and a list of key words.

5. Tables must be presented in an original typed or computer-printed form, instead of a photocopied version. **Numbers, totals, percentile data on the tables must coincide with those in the texts of the articles.** Tables and graphs must be headed.

6. Photographs are required to be contrasted and must be submitted with doubles. Please number each photograph with a pencil on its back, indicate author's name, title of the article (short version), and mark out its top and bottom parts. Drawings must be accurate, drafts and diagrams drawn in Indian ink (or black ink). Photocopies of the X-ray photographs must be presented in a positive image in **tiff format**.

Accurately numbered subtitles for each illustration must be listed on a separate sheet of paper. In the subtitles for the microphotographs please indicate the ocular and objective lens magnification power, method of coloring or impregnation of the microscopic sections (preparations).

7. Please indicate last names, first and middle initials of the native authors, present names and initials of the foreign authors in the transcription of the original language, enclose in parenthesis corresponding number under which the author is listed in the reference materials.

8. Please follow guidance offered to authors by The International Committee of Medical Journal Editors guidance in its Uniform Requirements for Manuscripts Submitted to Biomedical Journals publication available online at: http://www.nlm.nih.gov/bsd/uniform_requirements.html
http://www.icmje.org/urm_full.pdf
In GMN style for each work cited in the text, a bibliographic reference is given, and this is located at the end of the article under the title "References". All references cited in the text must be listed. The list of references should be arranged alphabetically and then numbered. References are numbered in the text [numbers in square brackets] and in the reference list and numbers are repeated throughout the text as needed. The bibliographic description is given in the language of publication (citations in Georgian script are followed by Cyrillic and Latin).

9. To obtain the rights of publication articles must be accompanied by a visa from the project instructor or the establishment, where the work has been performed, and a reference letter, both written or typed on a special signed form, certified by a stamp or a seal.

10. Articles must be signed by all of the authors at the end, and they must be provided with a list of full names, office and home phone numbers and addresses or other non-office locations where the authors could be reached. The number of the authors (co-authors) must not exceed the limit of 5 people.

11. Editorial Staff reserves the rights to cut down in size and correct the articles. Proof-sheets are not sent out to the authors. The entire editorial and collation work is performed according to the author's original text.

12. Sending in the works that have already been assigned to the press by other Editorial Staffs or have been printed by other publishers is not permissible.

Articles that Fail to Meet the Aforementioned Requirements are not Assigned to be Reviewed.

ავტორთა საყურადღებოდ!

რედაქციაში სტატიის წარმოდგენისას საჭიროა დავიცვათ შემდეგი წესები:

1. სტატია უნდა წარმოადგინოთ 2 ცალად, რუსულ ან ინგლისურ ენებზე,დაბეჭდილი სტანდარტული ფურცლის 1 გვერდზე, 3 სმ სიგანის მარცხენა ველისა და სტრიქონებს შორის 1,5 ინტერვალის დაცვით. გამოყენებული კომპიუტერული შრიფტი რუსულ და ინგლისურენოვან ტექსტებში - **Times New Roman (Кириллица)**, ხოლო ქართულენოვან ტექსტში საჭიროა გამოვიყენოთ **AcadNusx.** შრიფტის ზომა – 12. სტატიას თან უნდა ახლდეს CD სტატიით.

2. სტატიის მოცულობა არ უნდა შეადგენდეს 10 გვერდზე ნაკლებს და 20 გვერდზე მეტს ლიტერატურის სიის და რეზიუმეების (ინგლისურ, რუსულ და ქართულ ენებზე) ჩათვლით.

3. სტატიაში საჭიროა გაშუქდეს: საკითხის აქტუალობა; კვლევის მიზანი; საკვლევი მასალა და გამოყენებული მეთოდები; მიღებული შედეგები და მათი განსჯა. ექსპერიმენტული ხასიათის სტატიების წარმოდგენისას ავტორებმა უნდა მიუთითონ საექსპერიმენტო ცხოველების სახეობა და რაოდენობა; გაუტკივარებისა და დაძინების მეთოდები (მწვავე ცდების პირობებში).

4. სტატიას თან უნდა ახლდეს რეზიუმე ინგლისურ, რუსულ და ქართულ ენებზე არანაკლებ ნახევარი გვერდის მოცულობისა (სათაურის, ავტორების, დაწესებულების მითითებით და უნდა შეიცავდეს შემდეგ განყოფილებებს: მიზანი, მასალა და მეთოდები, შედეგები და დასკვნები; ტექსტუალური ნაწილი არ უნდა იყოს 15 სტრიქონზე ნაკლები) და საკვანძო სიტყვების ჩამონათვალი (key words).

5. ცხრილები საჭიროა წარმოადგინოთ ნაბეჭდი სახით. ყველა ციფრული, შემაჯამებელი და პროცენტული მონაცემები უნდა შეესაბამებოდეს ტექსტში მოყვანილს.

6. ფოტოსურათები უნდა იყოს კონტრასტული; სურათები, ნახაზები, დიაგრამები - დასათაურებული, დანომრილი და სათანადო ადგილას ჩასმული. რენტგენოგრამების ფოტოასლები წარმოადგინეთ პოზიტიური გამოსახულებით **tiff** ფორმატში. მიკროფოტოსურათების წარწერებში საჭიროა მიუთითოთ ოკულარის ან ობიექტივის საშუალებით გადიდების ხარისხი, ანათალების შეღებვის ან იმპრეგნაციის მეთოდი და აღნიშნოთ სურათის ზედა და ქვედა ნაწილები.

7. სამამულო ავტორების გვარები სტატიაში აღინიშნება ინიციალების თანდართვით, უცხოურისა – უცხოური ტრანსკრიპციით.

8. სტატიას თან უნდა ახლდეს ავტორის მიერ გამოყენებული სამამულო და უცხოური შრომების ბიბლიოგრაფიული სია (ბოლო 5-8 წლის სიღრმით). ანბანური წყობით წარმოდგენილ ბიბლიოგრაფიულ სიაში მიუთითეთ ჯერ სამამულო, შემდეგ უცხოელი ავტორები (გვარი, ინიციალები, სტატიის სათაური, ჟურნალის დასახელება, გამოცემის ადგილი, წელი, ჟურნალის №, პირველი და ბოლო გვერდები). მონოგრაფიის შემთხვევაში მიუთითეთ გამოცემის წელი, ადგილი და გვერდების საერთო რაოდენობა. ტექსტში კვადრატულ ფჩხილებში უნდა მიუთითოთ ავტორის შესაბამისი N ლიტერატურის სიის მიხედვით. მიზანშეწონილია, რომ ციტირებული წყაროების უმეტესი ნაწილი იყოს 5-6 წლის სიღრმის.

9. სტატიას თან უნდა ახლდეს: ა) დაწესებულების ან სამეცნიერო ხელმძღვანელის წარდგინება, დამოწმებული ხელმოწერითა და ბეჭდით; ბ) დარგის სპეციალისტის დამოწმებული რეცენზია, რომელშიც მითითებული იქნება საკითხის აქტუალობა, მასალის საკმაობა, მეთოდის სანდოობა, შედეგების სამეცნიერო-პრაქტიკული მნიშვნელობა.

10. სტატიის ბოლოს საჭიროა ყველა ავტორის ხელმოწერა, რომელთა რაოდენობა არ უნდა აღემატებოდეს 5-ს.

11. რედაქცია იტოვებს უფლებას შეასწოროს სტატია. ტექსტზე მუშაობა და შეჯერება ხდება საავტორო ორიგინალის მიხედვით.

12. დაუშვებელია რედაქციაში ისეთი სტატიის წარდგენა, რომელიც დასაბეჭდად წარდგენილი იყო სხვა რედაქციაში ან გამოქვეყნებული იყო სხვა გამოცემებში.

აღნიშნული წესების დარღვევის შემთხვევაში სტატიები არ განიხილება.

GEORGIAN MEDICAL NEWS
NO 3 (372) 2026

Содержание:

GEORGIAN MEDICAL NEWS
No 3 (372) 2026

QUANTITATIVE CT-BASED PREDICTION OF EARLY FIBROSIS-LIKE LUNG REMODELING IN ACUTE COVID-19: INTEGRATION WITH CLINICAL AND BIOMARKER CORRELATES

Talgat Muminov[1], Yevgeniya Filippenko[2], Akhmetzhan Sugraliyev[3], Shynar Ospanova[4], Saule Kassenova[5], Gulstan Yessetova[1], Anar Rakisheva[6], Sanzhar Ashimbekov[7], Axsaule Serikbaeva[1].

[1]S.D. Asfendiyarov Kazakh National Medical University (Pulmonology Department), Almaty, Kazakhstan.
[2]S.D. Asfendiyarov Kazakh National Medical University (Visual Diagnostics Department), Almaty, Kazakhstan.
[3]S.D. Asfendiyarov Kazakh National Medical University (Internal Diseases Department), Almaty, Kazakhstan.
[4]Medical Center "Beta", Almaty, Kazakhstan.
[5]Scientific Research Institute of Cardiology and Internal Diseases (Internal Medicine Department), Almaty, Kazakhstan.
[6]S.D. Asfendiyarov Kazakh National Medical University (Phthisiology Department), Almaty, Kazakhstan.
[7]LLP "ArPi Canon Medical Systems KZ", Astana, Kazakhstan.

Abstract.

Fibrosis-like lung remodeling is increasingly recognized as a clinically relevant consequence of coronavirus disease 2019 (COVID-19), yet factors associated with early structural remodeling during the acute phase remain incompletely characterized. We hypothesized that acute fibroinflammatory remodeling reflects an interaction between systemic inflammatory–coagulation activation and quantifiable parenchymal alterations detectable by automated CT morphometry. In this retrospective cohort study, 77 hospitalized patients with RT-PCR–confirmed COVID-19 pneumonia and fibrosis-like abnormalities on high-resolution CT were evaluated. Fibrosis severity was graded qualitatively (Grades 1–4) using a CT-adapted fibrosis scale. Automated lung segmentation and density-based analysis quantified regional fibrotic involvement and total lung volumes. Clinical characteristics and laboratory biomarkers were integrated with quantitative imaging metrics to assess associations with the severity of fibrosis-like remodeling across CT grades. Increasing fibrosis grade was associated with older age ($p = 0.012$), elevated absolute neutrophil count ($p = 0.038$), and higher fibrinogen levels ($p = 0.046$), supporting an association between inflammatory–coagulation pathways and early structural remodeling. In contrast, admission oxygenation, symptom burden, comorbidity prevalence, and in-hospital mortality were not significantly associated with fibrosis severity. Among qualitative CT findings, pleural effusion was observed exclusively in higher grades ($p = 0.003$). Quantitative morphometry demonstrated a stepwise increase in high-attenuation fibrotic lung burden (right lung: 14.3% to 35.3%, $p = 0.002$; left lung: 15.0% to 38.8%, $p = 0.001$), accompanied by progressive lung volume reduction ($p \leq 0.002$). These objective imaging biomarkers revealed structural differences across fibrosis grades that were not fully captured by clinical severity indices. Early fibrosis-like remodeling in acute COVID-19 was associated with older age and markers of systemic inflammatory–coagulopathic activation rather than with initial clinical severity alone. Quantitative CT morphometry provides reproducible structural biomarkers that may enhance evaluation of the severity of fibrosis-like lung remodeling and mechanistic understanding of post-viral lung remodeling. Prospective multicenter studies are required to further validate these imaging biomarkers.

Key words. COVID-19, quantitative CT, lung fibrosis, inflammatory biomarkers, coagulation, lung volume, fibroinflammatory remodeling.

Introduction.

The global coronavirus disease 2019 (COVID-19) pandemic has resulted in a substantial population of survivors with persistent pulmonary sequelae. Among these, fibrosis and fibrosis-like lung abnormalities have emerged as clinically relevant complications because of their potential long-term impact on respiratory function and health-related quality of life [1]. Persistent structural alterations following acute infection raise concerns regarding chronic pulmonary remodeling and functional impairment.

The reported prevalence of post-COVID fibrotic changes varies considerably across studies. Recent meta-analyses estimate pooled prevalence rates approaching 45%, with a wide range from 9% to 84%, reflecting heterogeneity in study design, patient populations, imaging timing, and diagnostic criteria [2,3]. Comparable post-infectious fibrotic changes have previously been described after severe acute respiratory syndrome coronavirus 1 and Middle East respiratory syndrome coronavirus infections, with reported frequencies of 62% and 33%, respectively [4,5]. These observations suggest a shared fibroinflammatory response following severe viral pneumonia.

Despite accumulating evidence, important knowledge gaps remain regarding determinants of fibrosis-like remodeling severity during the acute phase of COVID-19 and early indicators of its progression. Several circulating biomarkers—including Krebs von den Lungen-6 (KL-6), matrix metalloproteinase-7, and lipocalin-2—have been investigated as potential markers of fibroproliferative activity; however, their clinical utility and reproducibility remain uncertain [6-8]. High-resolution computed tomography (HRCT) remains the reference imaging modality for structural assessment of interstitial abnormalities and may provide additional value when combined with quantitative image analysis techniques [9,10].

Longitudinal data indicate that a subset of patients demonstrate persistent fibrosis-like abnormalities months to years after infection, and some continue to require respiratory support [11]. These findings underscore the need for early risk stratification and objective imaging-based quantification of lung remodeling

during hospitalization. A better understanding of clinical, laboratory, and quantitative imaging correlates may facilitate identification of patients at risk for more advanced fibrosis-like changes.

While prior studies have predominantly focused on long-term post-COVID fibrotic sequelae, determinants of fibrosis-like remodeling severity during the acute phase remain insufficiently characterized, particularly in the context of integrated quantitative imaging and systemic biomarker assessment. We hypothesized that acute-phase fibrosis-like lung remodeling reflects an interaction between inflammatory burden and structural parenchymal alterations that can be objectively captured using quantitative CT metrics.

Therefore, the present study aimed to evaluate associations between CT-derived morphometric parameters, clinical characteristics, and laboratory biomarkers with the severity of fibrosis-like lung remodeling and to explore differences between low-grade and high-grade remodeling patterns during hospitalization for acute COVID-19 pneumonia.

Materials and Methods.

Selection of patients:

This retrospective cohort study was approved by the Institutional Review Board, which waived the requirement for informed consent due to the use of de-identified data. Consecutive nonprobability sampling was applied.

Between 1 October and 2 December 2020, medical records of 798 consecutive patients admitted to a modular COVID-19 treatment facility affiliated with the I. Zhekenov City Clinical Infectious Diseases Hospital (Almaty, Kazakhstan) were reviewed. All cases were confirmed by reverse transcription–polymerase chain reaction (RT-PCR).

Patients were screened for the presence of fibrosis-like abnormalities on high-resolution CT (HRCT). The present analysis focused specifically on patients demonstrating fibrosis-like remodeling in order to evaluate clinical, laboratory, and imaging characteristics associated with the severity of these structural changes. According to predefined inclusion and exclusion criteria, 77 patients demonstrating fibrosis-like abnormalities on HRCT (40 men and 37 women; mean age 64.2 ± 10.2 years) were included in the final analysis (Figure 1).

Respiratory impairment was defined as peripheral oxygen saturation (SpO_2) ≤ 95% in combination with dyspnea at rest. Demographic variables included age, sex, smoking history, hospital length of stay, and in-hospital mortality. Clinical variables comprised presenting symptoms, oxygen saturation on admission, and documented comorbidities. Laboratory parameters included white blood cell count (WBC), absolute lymphocyte count (ALC), absolute neutrophil count (ANC), neutrophil-to-lymphocyte ratio (NLR), alanine aminotransferase (ALT), aspartate aminotransferase (AST), total serum protein, prothrombin time, and fibrinogen.

CT Acquisition Protocol:

All chest CT examinations were performed using a 64-slice scanner (Revolution EVO, GE Healthcare, USA). Acquisition parameters included a tube voltage of 120 kVp and tube current of 60–120 mAs with automatic exposure control. Images were acquired with a slice thickness of 1.25 mm and reconstructed at intervals of 1.0–3.0 mm. Scanning was performed in the supine position during full inspiration without intravenous contrast administration.

HRCT examinations were performed during hospitalization according to clinical indications. The interval between hospital admission and HRCT acquisition was recorded for all patients. HRCT was performed at a median of 6 days after hospital admission (IQR 4–9 days), corresponding approximately to 12 days after symptom onset and thus generally reflecting the organizing phase of COVID-19 pneumonia.

Qualitative CT Assessment:

CT images were reviewed independently by two thoracic radiologists with 10 and 37 years of experience, respectively, using both lung (window width 1500 HU; level −600 HU) and mediastinal (window width 400 HU; level 40 HU) settings. Both readers were blinded to clinical and laboratory data at the time of image interpretation. Discrepancies were resolved by consensus review.

Typical CT manifestations of COVID-19 pneumonia, including ground-glass opacities, bilateral peripheral lower-lobe predominance, and focal vascular enlargement, as well as less specific findings such as central involvement, crazy-paving pattern, fibrous streaks, reversed halo sign, pleural effusion, and mediastinal lymphadenopathy, were recorded for subsequent correlation analysis [12].

Global CT severity was visually assessed using a previously published semiquantitative lobar scoring system [13,14]. Each of the five lobes was assigned a score from 0 to 5 based on the estimated percentage of parenchymal involvement (1: 1–4%;

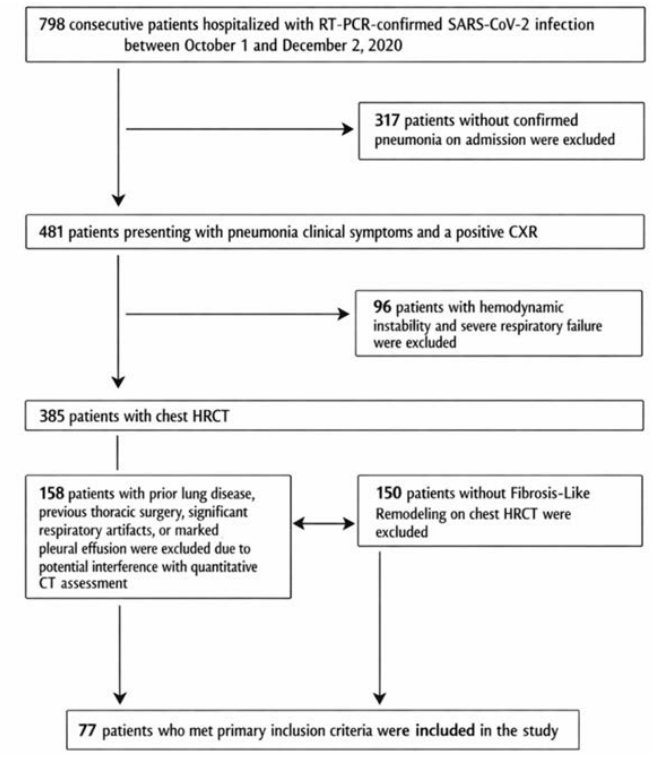

Figure 1. *Flowchart of patient selection based on clinical and HRCT criteria.*

2: 5–25%; 3: 26–49%; 4: 50–75%; 5: 76–100%). The total CT severity score (maximum 25 points) was multiplied by four to obtain a global percentage of lung involvement (maximum 100%). Severity categories were defined as CT severity grades: CT-1 (<25%), CT-2 (25–50%), CT-3 (50–75%), and CT-4 (>75%).

Fibrosis-Like Remodeling Grading:

Fibrosis-like abnormalities were graded using a CT-based semiquantitative scoring system adapted from the histologic fibrosis grading described by Ashcroft [15]. Grades were defined as follows: Grade 0: normal lung parenchyma; Grade 1: minimal fibrosis-like changes with alveolar or bronchiolar wall thickening; Grade 2: reticulation with interlobular and intralobular septal thickening; Grade 3: subpleural linear opacities or parenchymal bands; Grade 4: architectural distortion with associated volume loss. Only patients demonstrating fibrosis-like abnormalities on HRCT (Grades 1–4) were included in the severity-based analysis. For statistical analysis, patients were categorized into four ordinal fibrosis severity groups (Grades 1–4).

Quantitative CT Analysis:

Automated lung segmentation and density analysis were performed using commercially available software (Vitrea Lung Density Analysis, Vital Images, Canon Medical Systems, USA). Automated segmentation of the lungs was applied to obtain quantitative measurements of parenchymal density distribution and total lung volume. Lung parenchyma attenuation values were categorized into predefined HU intervals in accordance with established radiologic recommendations: −1000 to <−950 HU: emphysematous changes; −950 to −850 HU: hyperinflated lung; −850 to −700 HU: normal parenchyma; −700 to −200 HU: higher-attenuation parenchymal abnormalities compatible with fibrosis-like remodeling. These density intervals were applied to quantify regional lung composition and the relative proportion of higher-attenuation parenchymal abnormalities, as well as total lung volume. Color-coded density maps were generated to visualize the spatial distribution of parenchymal abnormalities.

Statistical Analysis.

Statistical analyses were performed using IBM SPSS Statistics (Version 26.0; IBM Corp., Armonk, NY, USA). Normality of continuous variables was assessed using the Shapiro–Wilk test. Data are presented as mean ± standard deviation or median (interquartile range), as appropriate. Group comparisons across fibrosis grades were conducted using one-way ANOVA or the Kruskal–Walli's test, depending on distribution. Categorical variables were analyzed using χ^2 or Fisher's exact tests. A two-sided p value < 0.05 was considered statistically significant.

Results.

Demographic and Clinical Characteristics:

A total of 77 patients with RT-PCR-confirmed COVID-19 pneumonia and fibrosis-like abnormalities on HRCT were included in the analysis. Baseline demographic and clinical characteristics stratified by fibrosis grade are presented in Table 1.

Age differed significantly across fibrosis grades (p = 0.012), with patients classified as Grade 2 and Grade 4 being older than those in Grade 3. No statistically significant differences were observed in sex distribution (p = 0.396). Oxygen saturation on admission was comparable among fibrosis grades (p = 0.264). Similarly, hospital length of stay did not differ significantly between groups (p = 0.667). The prevalence of at least one documented comorbidity was comparable across grades (p = 0.412). In-hospital mortality was low overall and did not significantly differ between groups (p = 0.292). Presenting symptoms, including fever, dyspnea at rest, and dry cough, occurred at similar frequencies across fibrosis grades (p range, 0.510–0.545).

Laboratory Findings:

Laboratory parameters on admission stratified by fibrosis grade are presented in Table 2.

ANC differed significantly across fibrosis grades (p = 0.038). Fibrinogen levels also demonstrated a statistically significant difference between groups (p = 0.046). In contrast, total WBC and NLR showed non-significant trends toward variation across grades (p = 0.079 and p = 0.080, respectively). No statistically significant differences were observed for ALC, ALT, AST, total serum protein, or prothrombin time (all p > 0.05).

CT Imaging Features:

CT imaging findings and the distribution of parenchymal abnormalities across HRCT fibrosis grades are presented in Table 3.

Among additional CT abnormalities, pleural effusion was the only feature that differed significantly across fibrosis grades (p = 0.003), and it was observed exclusively in patients classified as higher fibrosis grades. Other abnormalities—including the crazy-paving pattern, reversed halo sign, vascular enlargement, mediastinal lymphadenopathy, and diffuse alveolar damage—did not demonstrate statistically significant differences between groups (p range, 0.122–0.651). CT severity score categories (CT-1 to CT-4) were distributed comparably across fibrosis grades, with no statistically significant differences observed (p range, 0.163–0.858).

Quantitative Lung Morphometry by Fibrosis Grade:

Automated quantitative analysis of lung parenchyma was performed using Vitrea Lung Density Analysis software. Representative examples of density mapping and regional parenchymal classification across fibrosis grades are shown in (Figures 2-5).

Quantitative CT metrics demonstrated significant differences across fibrosis grades (Figure 6 and Table 4). The percentage of fibrotic lung involvement increased progressively from Grade 1 to Grade 4. For the right lung, mean fibrotic involvement was 14.3 ± 5.4%, 25.2 ± 12.9%, 25.3 ± 13.2%, and 35.3 ± 10.7%, respectively (p = 0.002). For the left lung, corresponding values were 15.0 ± 5.8%, 24.4 ± 12.8%, 25.0 ± 12.1%, and 38.8 ± 11.1%, respectively (p = 0.001).

Box-and-whisker plots with overlaid individual data points illustrate the distribution of quantitative CT-derived metrics across fibrosis grades. Progressive increases in fibrosis-like lung involvement and corresponding reductions in total lung volume are shown from Grade 1 to Grade 4. Quantitative measurements

Table 1. *Baseline Demographic and Clinical Characteristics According to HRCT Fibrosis Grade.*

Variable	Grade 1 (n = 9)	Grade 2 (n = 14)	Grade 3 (n = 44)	Grade 4 (n = 10)	p Value
Age, years (mean ± SD)	64.4 ± 7.6	69.9 ± 8.6	61.1 ± 10.3	69.6 ± 9.4	0.012*
Male sex, n (%)	4 (44.4)	10 (71.4)	22 (50.0)	4 (40.0)	0.396
SpO_2 on admission, % (mean ± SD)	93.2 ± 3.5	88.6 ± 8.4	91.3 ± 6.3	90.7 ± 2.7	90.7 ± 2.7
Hospital length of stay, days (mean ± SD)	11.0 ± 2.2	13.8 ± 6.6	11.8 ± 6.9	13.1 ± 7.6	0.667
Any comorbidity**, n (%)	5 (55.5)	10 (71.4)	32 (72.7)	8 (80.0)	0.412
In-hospital mortality, n (%)	1 (11.1)	3 (21.4)	2 (4.5)	1 (10.0)	0.292
Fever at admission, n (%)	3 (33.3)	4 (28.6)	21 (47.7)	5 (50.0)	0.545
Dyspnea at rest, n (%)	7 (77.8)	9 (64.3)	26 (59.1)	8 (80.0)	0.510
Dry cough, n (%)	7 (77.8)	11 (78.6)	36 (81.8)	6 (60.0)	0.520

SD, standard deviation; SpO_2, peripheral oxygen saturation. **Statistically significant at $p < 0.05$.* **Any comorbidity includes hypertension, ischemic heart disease, diabetes mellitus, and prior stroke. Continuous variables were compared using one-way ANOVA or Kruskal–Wallis tests, as appropriate; categorical variables were compared using χ^2 or Fisher's exact tests.

Table 2. *Laboratory Parameters on Admission According to HRCT Fibrosis Grade.*

Laboratory Parameter	Grade 1 (n = 9)	Grade 2 (n = 14)	Grade 3 (n = 44)	Grade 4 (n = 10)	p Value
WBC, $\times 10^9$/L (mean ± SD)	6.3 ± 2.9	7.7 ± 2.6	6.0 ± 3.2	7.5 ± 5.5	0.079
ALC, $\times 10^9$/L (mean ± SD)	3.3 ± 3.8	1.2 ± 0.7	1.1 ± 0.5	1.0 ± 0.4	0.118
ANC, $\times 10^9$/L (mean ± SD)	5.3 ± 2.8	6.0 ± 2.6	4.3 ± 3.1	5.5 ± 5.0	0.038*
NLR (mean ± SD)	2.6 ± 1.6	7.4 ± 5.7	4.1 ± 2.9	5.8 ± 4.9	0.080
ALT, U/L (mean ± SD)	57.7 ± 42.6	35.7 ± 26.1	47.1 ± 51.0	40.4 ± 41.5	0.501
AST, U/L (mean ± SD)	35.7 ± 14.7	31.8 ± 13.8	43.8 ± 39.1	43.8 ± 23.6	0.527
Total protein, g/L (mean ± SD)	65.6 ± 5.0	66.9 ± 7.2	68.5 ± 6.0	69.7 ± 5.1	0.162
Prothrombin time, s (mean ± SD)	13.8 ± 2.0	13.2 ± 2.6	13.9 ± 4.7	14.5 ± 6.4	0.598
Fibrinogen, g/L (mean ± SD)	3.7 ± 0.8	5.2 ± 1.3	4.7 ± 2.2	3.8 ± 1.8	0.046*

WBC, white blood cell count; ALC, absolute lymphocyte count; ANC, absolute neutrophil count; NLR, neutrophil-to-lymphocyte ratio; ALT, alanine aminotransferase; AST, aspartate aminotransferase; SD, standard deviation. *Statistically significant at $p < 0.05$. Continuous variables were compared using one-way ANOVA or Kruskal–Wallis tests, as appropriate.

Table 3. *Distribution of CT Parenchymal Abnormalities According to HRCT Fibrosis Grade.*

Feature	Grade 1 (n = 9)	Grade 2 (n = 14)	Grade 3 (n = 44)	Grade 4 (n = 10)	p Value
GGO Distribution					
Bilateral	9 (100.0)	14 (100.0)	43 (97.7)	10 (100.0)	0.842
Unilateral	0 (0.0)	0 (0.0)	1 (2.3)	0 (0.0)	0.677
Peripheral predominance	8 (88.9)	14 (100.0)	44 (100.0)	10 (100.0)	0.562
Central involvement	7 (77.8)	13 (92.9)	40 (90.9)	9 (90.0)	0.514
Additional CT Features					
Crazy-paving pattern	6 (66.7)	8 (57.1)	20 (45.5)	5 (50.0)	0.651
Reversed halo sign	1 (11.1)	0 (0.0)	1 (2.3)	0 (0.0)	0.357
Vascular enlargement	6 (66.7)	12 (85.7)	40 (90.9)	10 (100.0)	0.122
Pleural effusion	0 (0.0)	0 (0.0)	0 (0.0)	2 (20.0)	0.003*
Mediastinal lymphadenopathy	5 (55.6)	6 (42.9)	30 (68.2)	6 (60.0)	0.390
Diffuse alveolar damage	0 (0.0)	0 (0.0)	2 (4.5)	1 (10.0)	0.577
CT Severity Score Category					
CT-1	2 (22.2)	3 (21.4)	4 (9.1)	0 (0.0)	0.276
CT-2	5 (55.6)	4 (28.6)	17 (38.6)	2 (20.0)	0.383
CT-3	2 (22.2)	5 (35.7)	14 (31.8)	4 (40.0)	0.858
CT-4	0 (0.0)	2 (14.3)	9 (20.5)	4 (40.0)	0.858

GGO, ground-glass opacity. *Statistically significant at $p < 0.05$. Categorical variables were compared using χ^2 or Fisher's exact tests, as appropriate.

Table 4. *Quantitative Fibrotic Involvement and Lung Volumes According to HRCT Fibrosis Grade.*

Parameter	Grade 1 (n = 9)	Grade 2 (n = 14)	Grade 3 (n = 44)	Grade 4 (n = 10)	p Value
Right lung fibrosis, %(mean ± SD)	14.3 ± 5.4	25.2 ± 12.9	25.3 ± 13.2	35.3 ± 10.7	0.002*
Left lung fibrosis, % (mean ± SD)	15.0 ± 5.8	24.4 ± 12.8	25.0 ± 12.1	38.8 ± 11.1	0.001*
Right lung volume, mL (mean ± SD)	2612 ± 743	2253 ± 506	2127 ± 571	1645 ± 535	0.001*
Left lung volume, mL (mean ± SD)	2178 ± 581	2067 ± 527	1914 ± 519	1304 ± 387	0.002*

SD, standard deviation. *Statistically significant at $p < 0.05$. Continuous variables were compared using one-way ANOVA or Kruskal–Wallis tests, as appropriate.

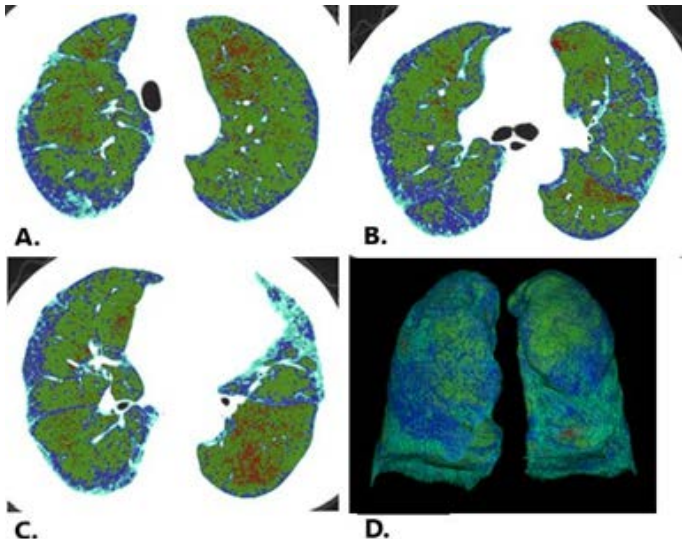

Figure 2. *Grade 1: Automated Lung Density Color Mapping. Axial CT images obtained (A) 5 cm above the tracheal bifurcation, (B) at the level of the tracheal bifurcation, and (C) 5 cm below the tracheal bifurcation, with (D) three-dimensional volume rendering. Density-based color classification according to HU intervals: red, emphysema (−1000 to −950 HU); green, hyperinflation (−949 to −850 HU); blue, normal parenchyma (−849 to −700 HU); light blue, hypoventilation/ consolidation corresponding to fibrosis-like changes (−699 to −200 HU).*

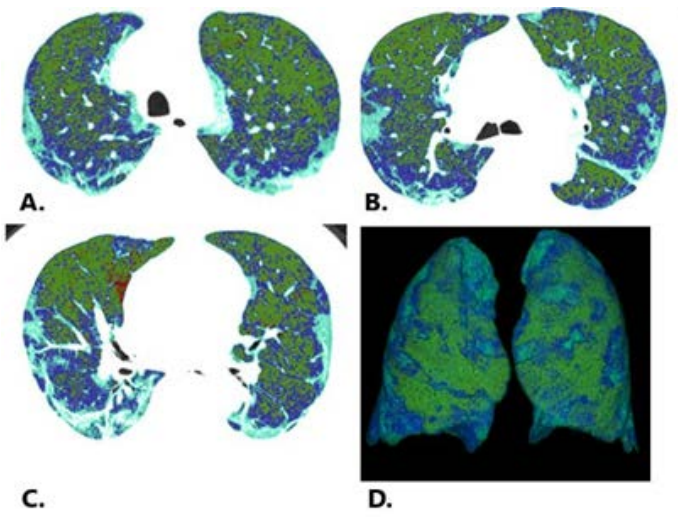

Figure 3. *Grade 2: Automated Lung Density Color Mapping. Axial CT images obtained (A) 5 cm above the tracheal bifurcation, (B) at the level of the tracheal bifurcation, and (C) 5 cm below the tracheal bifurcation, with (D) three-dimensional volume rendering. Density-based color classification according to HU intervals: red, emphysema (−1000 to −950 HU); green, hyperinflation (−949 to −850 HU); blue, normal parenchyma (−849 to −700 HU); light blue, hypoventilation/ consolidation corresponding to fibrosis-like changes (−699 to −200 HU).*

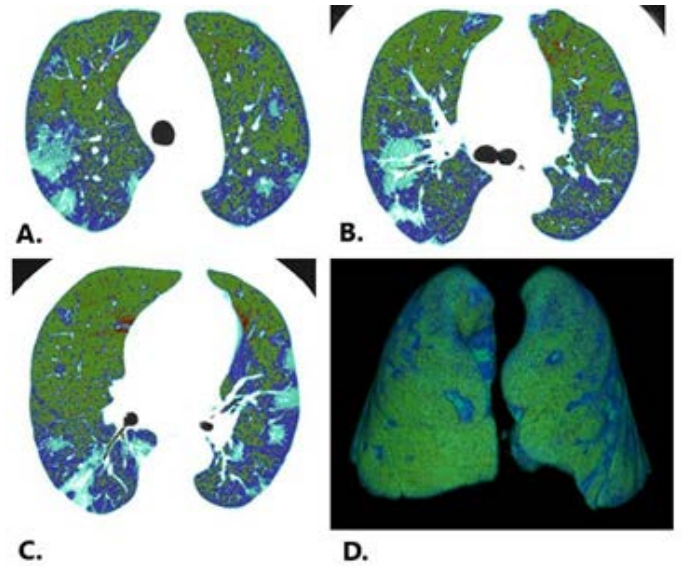

Figure 4. *Grade 3: Automated Lung Density Color Mapping. Axial CT images obtained (A) 5 cm above the tracheal bifurcation, (B) at the level of the tracheal bifurcation, and (C) 5 cm below the tracheal bifurcation, with (D) three-dimensional volume rendering. Density-based color classification according to HU intervals: red, emphysema (−1000 to −950 HU); green, hyperinflation (−949 to −850 HU); blue, normal parenchyma (−849 to −700 HU); light blue, hypoventilation/ consolidation corresponding to fibrosis-like changes (−699 to −200 HU).*

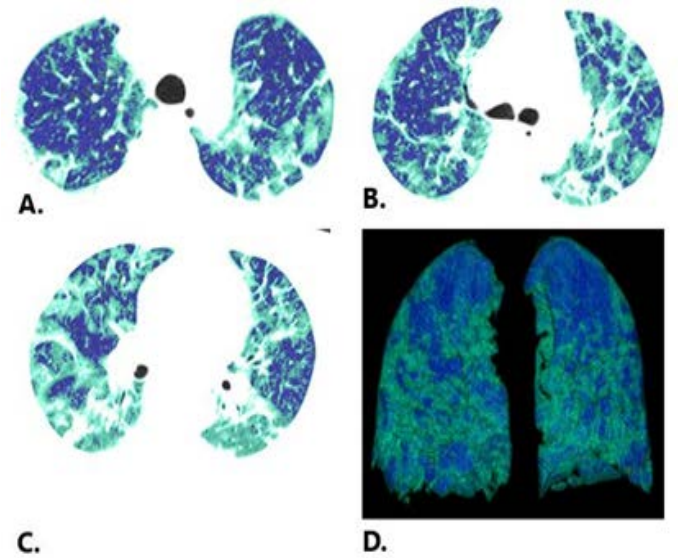

Figure 5. *Grade 4: Automated Lung Density Color Mapping. Axial CT images obtained (A) 5 cm above the tracheal bifurcation, (B) at the level of the tracheal bifurcation, and (C) 5 cm below the tracheal bifurcation, with (D) three-dimensional volume rendering. Density-based color classification according to HU intervals: red, emphysema (−1000 to −950 HU); green, hyperinflation (−949 to −850 HU); blue, normal parenchyma (−849 to −700 HU); light blue, hypoventilation/ consolidation corresponding to fibrosis-like changes (−699 to −200 HU).*

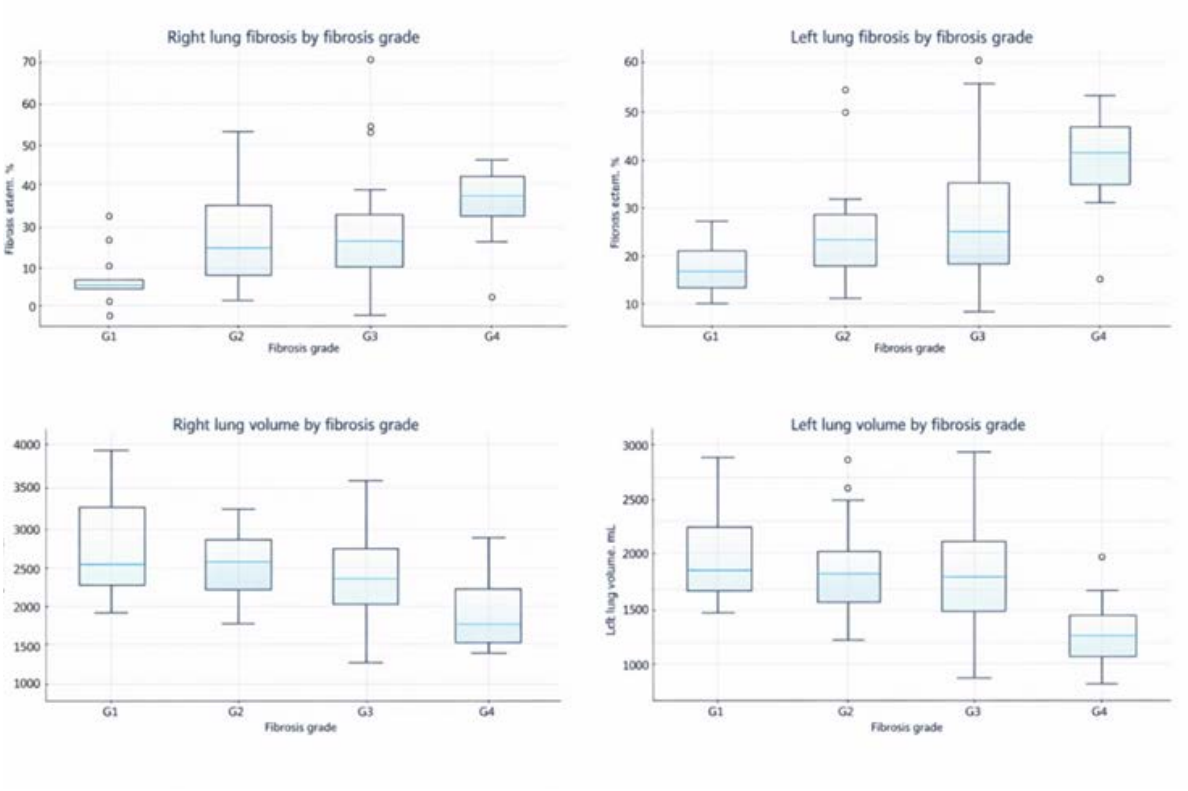

Figure 6. *Quantitative CT Metrics Across Fibrosis-Like Grades.*

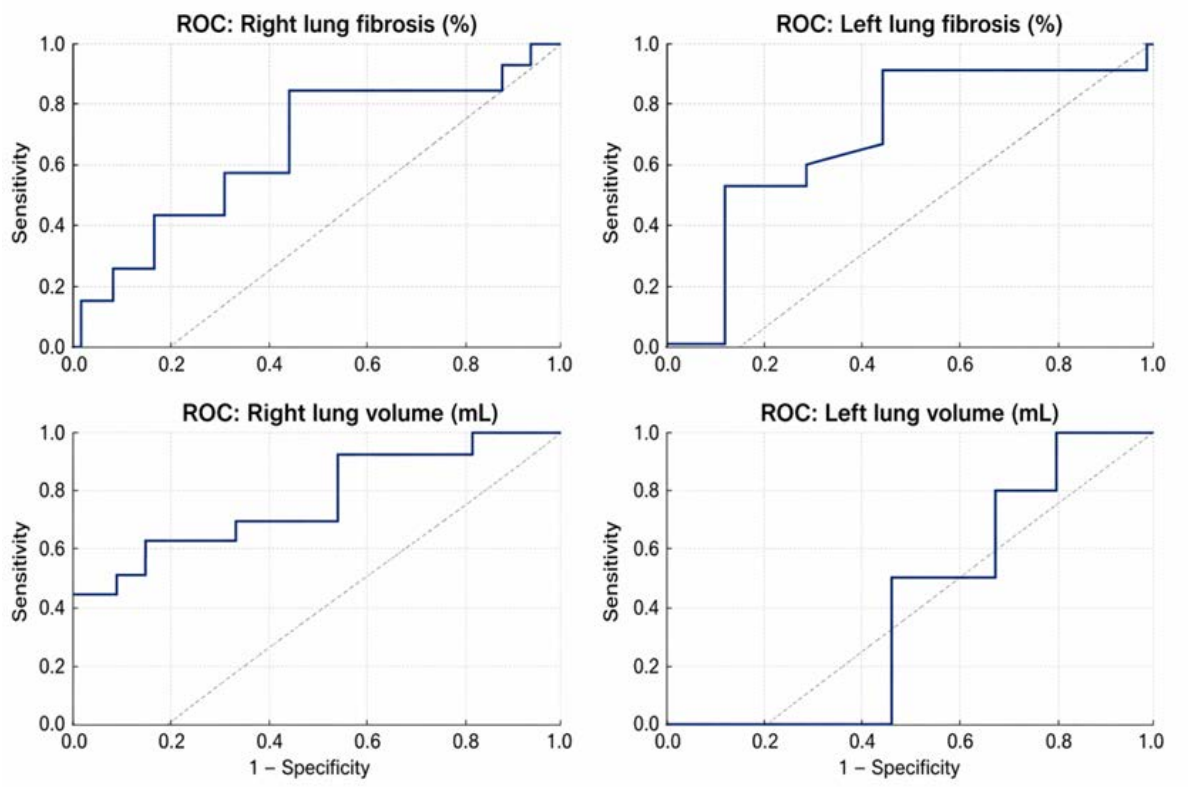

Figure 7. *ROC curves of right lung fibrosis (%), left lung fibrosis (%), right lung volume (mL), and left lung volume (mL) for discrimination between low-grade (Grades 1–2) and high-grade (Grades 3–4) fibrosis-like remodeling.*

Table 5. *Discriminatory Performance of Clinical, Laboratory, and Quantitative CT Parameters for Differentiating High-Grade Fibrosis-like Remodeling (Grades 3–4) from Low-Grade Remodeling (Grades 1–2) in Patients with Acute COVID-19 Pneumonia.*

Parameter	AUC	AUC 95% CI	Optimal cut-off*	Sensitivity	Specificity	PPV	NPV	Accuracy
Age (years)	0.76	0.54-0.94	0.68	0.82	0.71	0.88	0.62	0.79
Fibrinogen (g/L)	0.43	0.17-0.71	0.73	0.12	1.00	1.00	0.32	0.38
ANC (×10⁹/L)	0.71	0.46-0.95	0.65	0.88	0.71	0.88	0.71	0.83
NLR	0.50	0.14-0.83	0.63	0.94	0.43	0.80	0.75	0.79
Right lung fibrosis (%)	0.66	0.36-0.91	0.60	0.88	0.57	0.83	0.67	0.79
Left lung fibrosis (%)	0.74	0.45–0.95	0.58	0.94	0.57	0.84	0.80	0.83
Right lung volume (mL)**	0.82	0.61–0.97	0.70	0.59	1.00	1.00	0.50	0.71
Left lung volume (mL)**	0.11	0.00–0.29	1.78	0.00	1.00	—	0.29	0.29
Integrated model***	0.59	0.32–0.84	0.64	0.59	0.71	0.83	0.42	0.62

ANC, absolute neutrophil count; AUC, area under the receiver operating characteristic curve; CI, confidence interval; PPV, positive predictive value; NLR, neutrophil-to-lymphocyte ratio; NPV, negative predictive value.
* Optimal cut-offs based on Youden's index (calculated on held-out test data).
** For lung volume, higher values are associated with lower fibrosis severity; cut-off values correspond to normalized predicted probabilities, not raw milliliter thresholds.
***Integrated model includes age, fibrinogen, ANC, NLR, bilateral fibrosis percentages, and right and left lung volumes (multivariable logistic regression).

were obtained using automated lung density morphometry (Vitrea Lung Density Analysis software).

Total lung volume decreased progressively across fibrosis grades. Mean right lung volume declined from 2612 ± 743 mL in Grade 1 to 1645 ± 535 mL in Grade 4 ($p = 0.009$). Similarly, mean left lung volume decreased from 2178 ± 581 mL to 1304 ± 387 mL across the same grades ($p = 0.002$).

ROC Analysis and Discriminatory Performance of Clinical and Quantitative CT Parameters:

Quantitative CT metrics, particularly fibrosis percentage and right lung volume, demonstrated moderate-to-good discriminatory performance for differentiating between low-grade and high-grade fibrosis-like remodeling, whereas left lung volume showed limited discriminative ability (Figure 7).

To further evaluate the combined contribution of clinical, laboratory, and imaging variables, a multivariable logistic regression model was constructed incorporating age, absolute neutrophil count (ANC), fibrinogen, neutrophil-to-lymphocyte ratio (NLR), and quantitative CT parameters. The integrated model demonstrated limited overall discriminatory performance, with an AUC of 0.59 (95% CI, 0.32–0.84).

At an optimized probability threshold of 0.64, the model achieved a specificity of 0.71 and a positive predictive value (PPV) of 0.83, indicating greater ability to identify patients with high-grade fibrosis-like remodeling than to exclude lower-grade cases (Table 5).

In summary, increasing fibrosis-like grade was associated with older age, higher ANC, and elevated fibrinogen levels. Quantitative CT analysis demonstrated progressive increases in fibrotic lung involvement accompanied by corresponding reductions in total lung volume across fibrosis grades. Among qualitative CT features, pleural effusion was the only abnormality that differed significantly between groups.

Discussion.

In this cohort of hospitalized patients with acute COVID-19 pneumonia and fibrosis-like abnormalities on HRCT, higher grades of fibrosis-like remodeling were associated with differences in age and selected inflammatory and coagulation biomarkers, whereas initial clinical presentation, oxygenation status, and in-hospital outcomes did not demonstrate significant associations. The absence of a clear relationship between hypoxemia, symptom burden, or hospital length of stay and fibrosis grade suggests that early fibroinflammatory remodeling may occur independently of the severity of acute clinical manifestations. Similar dissociation between clinical status and persistent CT abnormalities has been described in longitudinal studies of post-COVID lung disease [16,17].

Among laboratory biomarkers, elevated absolute neutrophil count and fibrinogen levels differed significantly across fibrosis grades. Neutrophil activation and neutrophil extracellular trap–mediated endothelial injury have been implicated in COVID-19–related microvascular dysfunction and aberrant tissue repair, providing a potential mechanistic framework linking inflammatory activity with structural lung changes [18,19]. Elevated fibrinogen reflects both systemic inflammation and hypercoagulability, processes that may accompany fibroinflammatory tissue responses [20,21]. However, these markers represent nonspecific indicators of systemic inflammatory and coagulation activity, and their association with fibrosis-like remodeling should therefore be interpreted cautiously. These biomarkers may therefore reflect the intensity of the acute inflammatory response and host immune activation during infection rather than fibrosis-specific biological pathways.

Qualitative imaging analysis demonstrated that the distribution of ground-glass opacities—including laterality, peripheral versus central predominance, and lobar involvement—did not differ significantly across fibrosis grades. These patterns are generally considered markers of acute alveolar injury rather than indicators of structural remodeling severity [22,23]. Additional CT features, including crazy-paving pattern, reversed halo sign, vascular enlargement, and mediastinal lymphadenopathy, were similarly distributed among groups. In contrast, pleural effusion

was observed exclusively in patients with higher fibrosis grades, consistent with prior reports linking pleural effusion to more severe inflammatory burden and vascular injury in COVID-19 pneumonia [26-28]. Although this observation requires validation, it may reflect more extensive interstitial injury in these patients.

Quantitative CT morphometry demonstrated progressive increases in fibrosis-like lung involvement accompanied by proportional reductions in total lung volume from Grade 1 to Grade 4. These findings provide objective densitometric evidence of structural remodeling and associated reductions in aerated lung volume. Previous studies have likewise reported reduced lung volumes and increased high-attenuation lung tissue in patients with persistent post-COVID radiologic abnormalities [9,10]. Automated quantitative analysis may therefore complement qualitative assessment by detecting subtle reticulation and regional volume changes that are less readily appreciated visually [29-31].

The integrated multivariable logistic regression model demonstrated limited discriminatory performance for differentiating low-grade from high-grade fibrosis-like remodeling. The relatively wide confidence interval likely reflects the modest sample size and heterogeneity within fibrosis subgroups. These findings should therefore be interpreted as exploratory and hypothesis-generating rather than as evidence of a robust classification model.

Collectively, the present findings suggest that fibrosis-like remodeling observed during the acute phase of COVID-19 pneumonia appears to be associated with patient age and markers of systemic inflammatory–coagulation activity, whereas acute clinical severity alone does not appear to fully explain the extent of structural lung changes. Integration of quantitative CT metrics with selected laboratory biomarkers may facilitate more comprehensive characterization of fibrosis-like remodeling severity during hospitalization. Prospective studies with longitudinal imaging follow-up will be required to clarify the temporal evolution and clinical implications of these remodeling patterns.

Conclusions.

In hospitalized patients with acute COVID-19 pneumonia, fibrosis-like lung remodeling on CT was associated with older age, neutrophil predominance, elevated fibrinogen levels, and quantitative reductions in lung volume. The integrated multiparametric model demonstrated limited correlates performance within this cohort and should be considered exploratory. These findings suggest a complementary role for quantitative CT morphometry and selected systemic biomarkers in the early structural characterization of fibrosis-like lung remodeling during the acute phase of COVID-19. Prospective validation in larger cohorts is required to confirm these observations and clarify their clinical implications.

Strengths and Limitations.

This study integrates qualitative HRCT assessment with automated quantitative CT morphometry and systemic laboratory biomarkers, providing a comprehensive and multidimensional evaluation of fibrosis-like lung remodeling during the acute phase of COVID-19. The application of standardized CT-based grading criteria combined with objective densitometric analysis enhances methodological consistency and helps reduce potential subjective bias in image interpretation. Moreover, the focus on early in-hospital imaging enables assessment of lung remodeling processes at a clinically relevant stage of disease evolution, which may contribute to improved early risk stratification. Nevertheless, several limitations should be acknowledged. First, the retrospective single-center design and the relatively small sample size, particularly within certain fibrosis grades, may limit the generalizability of the findings. Second, the timing of CT examinations was not fully standardized and was determined by clinical indications, which may have contributed to variability in imaging results. However, the interval between hospital admission and HRCT acquisition in our cohort was recorded (median 6 days, IQR 4–9 days), allowing an approximate estimation of the disease phase at the time of imaging. Third, the absence of histopathologic confirmation limits the ability of CT-based grading to fully characterize the underlying fibroinflammatory processes. Furthermore, the absence of a non-fibrosis control group limits the ability to evaluate factors associated with the development of fibrosis-like abnormalities, and therefore the present analysis focuses specifically on differences in remodeling severity among patients already demonstrating fibrosis-like changes on HRCT. In addition, the correlative model was not externally validated and therefore requires confirmation in larger independent cohorts. Finally, due to the observational nature of the study, causal relationships between inflammatory biomarkers and structural lung remodeling cannot be definitively established.

Acknowledgments.

The authors express their gratitude for the administrative and technical support provided by S.D. Asfendiyarov Kazakh National Medical University.

Conflicts of interest statement.

The authors declare no conflict of interest.

Funding.

This research was funded by the Science Committee of the Ministry of Science and Higher Education of the Republic of Kazakhstan (Grant No. AP14870557).

REFERENCES

1. Nalbandian A, Sehgal K, Gupta A, et al. Post-acute COVID-19 syndrome. Nat Med. 2021;27:601-615.
2. Shah AS, Wong AW, Hague CJ, et al. A prospective study of post-COVID fibrosis. Ann Am Thorac Soc. 2021;18:1007-1019.
3. Ahmed H, Patel K, Greenwood DC, et al. Long-term clinical outcomes in survivors of COVID-19. Clin Med (Lond). 2021;21:e30-e38.
4. Ong KC, Ng AW, Lee LS, et al. Pulmonary function and exercise capacity after severe acute respiratory syndrome. Chest. 2005;128:139-145.
5. Das KM, Lee EY, Singh R, et al. Follow-up chest radiographic findings in patients with MERS-CoV pneumonia. Clin Radiol. 2017;72:380-387.

6. d'Alessandro M, Bergantini L, Cameli P, et al. Serum KL-6 in COVID-19-related interstitial lung disease. Respir Res. 2021;22:1-9.
7. Wynne R, Atkinson C, Hume E, et al. Matrix metalloproteinase-7 and fibroblast markers in COVID-19. Thorax. 2022;77:349-358.
8. Chen Y, Chen W, Zhou J, et al. Lipocalin-2 in COVID-19–associated fibroproliferation. J Infect. 2021;83:98-105.
9. Yu M, Liu Y, Xu D, et al. Quantitative CT assessment of post-COVID-19 sequelae. Radiology. 2022;306:E167-E176.
10. Vasallo P, Grassi R, Arcadi T, et al. Quantitative CT analysis of persistent lung abnormalities after COVID-19. Eur Respir J. 2023;61:2200824.
11. Bellan M, Soddu D, Balbo PE, et al. Respiratory outcomes after COVID-19 hospitalization: a 4-year follow-up. Respir Res. 2021;22:1-10.
12. Adams HJA, Kwee TC, Yakar D, et al. Chest CT imaging signature of coronavirus disease 2019 infection. Chest. 2020;158:1885-1895.
13. Inui S, Fujikawa A, Jitsu M, et al. Chest CT findings in cases from the cruise ship Diamond Princess with COVID-19. Radiol Cardiothorac Imaging. 2020;2:e200110.
14. Sinitsyn VE, Tyurin IE, Mitkov VV. Role of imaging in diagnosis of COVID-19 pneumonia: consensus guidelines. J Radiol Nucl Med. 2020;101:72-89.
15. Ashcroft T, Simpson JM, Timbrell V. Simple method of estimating severity of pulmonary fibrosis on a numerical scale. J Clin Pathol. 1988;41:467-470.
16. Han X, Fan Y, Alwalid O, et al. Six-month follow-up chest CT findings after severe COVID-19 pneumonia. Radiology. 2021;299:E177-E186.
17. Myall KJ, Mukherjee B, Castanheira AM, et al. Persistent post-COVID-19 interstitial lung disease. Lancet Respir Med. 2021;9:601-612.
18. Middleton EA, He X, Denorme F, et al. Neutrophil extracellular traps contribute to immunothrombosis in COVID-19 ARDS. Nat Commun. 2020;11:3580.
19. Zuo Y, Yalavarthi S, Shi H, et al. Neutrophil extracellular traps in COVID-19. JCI Insight. 2020;5:e138999.
20. Schaefer L, Babelova A, Kiss E, et al. The matrix component fibrinogen triggers fibroblast activation via TLR4. Nat Commun. 2017;8:14815.
21. Fogarty H, Townsend L, Ni Cheallaigh C, et al. COVID-19 coagulopathy in critically ill patients. Br J Haematol. 2021;193:1020-1025.
22. Shi H, Han X, Jiang N, et al. Radiological findings from 81 patients with COVID-19 pneumonia. Radiology. 2020;296:E32-E40.
23. Bernheim A, Mei X, Huang M, et al. Chest CT findings in coronavirus disease 2019. Radiology. 2020;295:200-207.
24. de Sales AR, Viana AO, Lemos AC, et al. The reversed halo sign in COVID-19 pneumonia. J Bras Pneumol. 2020;46:e20200164.
25. Gbadamosi WA, Yusuf J, Okechukwu I, et al. Crazy-paving pattern in COVID-19 pneumonia. Clin Case Rep. 2022;10:e05953.
26. Xie X, Zhong Z, Zhao W, et al. Chest CT and clinical progression of COVID-19 pneumonia. Radiology. 2020;296:E15-E23.
27. Chung M, Bernheim A, Mei X, et al. CT imaging features of coronavirus disease 2019. Radiology. 2020;295:52-60.
28. Li K, Wu J, Wu F, et al. Chest CT findings in COVID-19 pneumonia: correlation with clinical features. Lancet Respir Med. 2020;8:475-481.
29. Jacob J, Bartholmai BJ, Rajagopalan S, et al. Mortality prediction in idiopathic pulmonary fibrosis using quantitative CT. Radiology. 2017;283:252-260.
30. Humphries SM, Swenson ER, Baird G, et al. CT biomarkers for lung disease quantification. Radiographics. 2020;40:1729-1744.
31. Bartholmai BJ, Raghunath S, Karwoski RA, et al. Quantitative CT imaging in interstitial lung disease. Eur Respir J. 2013;42:486-494.
32. Wei J, Yang H, Lei P, et al. Long-term lung volume changes after COVID-19 pneumonia. Clin Radiol. 2021;76:473.e1-473.e8.
33. Wang J, Hajizadeh N, Moore EE, et al. NET-mediated lung injury in COVID-19. Am J Respir Crit Care Med. 2020;201:992-1001.
34. Spadaro S, Park M, Turrini C, et al. Biomarkers of fibroproliferation in ARDS and COVID-19. Lancet Respir Med. 2021;9:691-702.